The effect of working fluid and compressibility on the optimal solidity of axial turbine cascades

Tosto, F.; Pini, M.; Colonna, Piero

Publication date
2024

Document Version
Final published version

Published in
Proceedings of the 6th International Seminar on ORC Power Systems

The effect of working fluid and compressibility on the optimal solidity in ORC turbine cascades

Francesco Tosto[1], David Pasquale[2], Piero Colonna[1], Matteo Pini[1*]

[1] Propulsion and Power, Delft University of Technology,
Kluyverweg 1, 2629 HS Delft
m.pini@tudelft.nl

[2] Turboden S.p.A.,
via Cernaia 10, 25124 Brescia,
Italy

* Corresponding Author

ABSTRACT

The blade solidity, namely the blade chord-to-pitch ratio, largely affects the fluid-dynamic performance of turbomachinery. For turbo-machines operating with air or steam, the optimal value of the solidity which maximizes the efficiency is estimated with empirical correlations such as the ones proposed by Zweifel (1945) and Traupel (1966). However, if the turbomachine operates with unconventional fluids, the accuracy of these correlations becomes questionable. Examples of such working fluids are the non-ideal (dense) vapors of organic compounds (e.g., hydrocarbons, siloxanes) used to operate organic Rankine cycle (ORC) power systems. This study investigates the effect of both the working fluid and the flow compressibility on the optimum pitch-to-chord ratio of turbine stages. A first principle model for the profile losses is developed for this purpose. Charts providing the optimal pitch-to-chord ratio for unconventional turbine stages are then provided. Numerical simulations of the flow over a turbine stator cascade have been conducted to validate the model results and evaluate the influence of both working fluid, flow compressibility, and solidity value on the loss breakdown. The results show that the optimal solidity of turbine cascades value significantly increases with the flow compressibility. Therefore, models providing the optimal solidity based on the estimate of passage loss only are not suited for unconventional turbines.

1. INTRODUCTION

The value of the blade solidity, i.e., the ratio c_x/s between the chord and the pitch, strongly affects the design and the performance of axial turbines. To reduce the weight and cost of the machine, high blade spacing and low solidity values are desired. However, efficient flow turning requires a sufficient number of blades. For low solidity values, the blade loading is high, causing poor fluid guidance and, therefore, flow separation over the rear suction side. Conversely, for high solidity values, the large cascade wetted area induces considerable passage losses. In summary, there is an optimum value of the axial solidity that minimizes the passage loss. In axial turbines operating with air or steam, this value is estimated through the empirical correlations proposed by Zweifel (1945) and Traupel (1966). The use of Zweifel's criterion is well documented also in recent literature (see, e.g., Giuffré and Pini, 2021) and the model, in its most general form, reads

$$Z_{\text{Zw}} = \frac{\text{actual blade loading}}{\text{ideal blade loading}} = \frac{\rho V_x (V_{y2} - V_{y1})}{(p_{t1} - p_2)\sigma_x}, \tag{1}$$

where ρ is the fluid density, p_{t1} the inlet total pressure, p_2 the outlet static pressure, V_{y1} and V_{y2} the tangential velocities at inlet and outlet, respectively, V_x the average axial velocity. Z_{Zw} is a coefficient whose value ranges between 0.8 and 1.1 depending on the type of turbine, e.g., $Z_{Zw} \sim 1.1$ in low pressure turbine stages of modern aircraft engines.

However, in non-conventional turbines for ORC or supercritical carbon dioxide power systems, the accuracy of Zweifel's criterion has not been thoroughly assessed yet. Furthermore, no design guidelines for the selection of the optimal solidity in unconventional turbomachinery is documented in the literature. To the authors' knowledge, the only study on the accuracy of the Zweifel's correlation is that of Doughty et al. (1992), who performed an experimental campaign on transonic stator cascades. They found that the Zweifel loading coefficient estimated from their experimental data was significantly higher than the value commonly used to design high pressure turbine nozzles.

Both Traupel and Zweifel's correlations take into account only the passage loss in the estimation of the optimal solidity. No effects of either wake mixing or shock losses are considered. Moreover, in non-conventional turbines, the high complexity of the working fluid molecules causes additional difficulties. The low value of the speed of sound typical of organic fluids induces high flow compressibility, as well as non-ideal gas effects, because the nozzle of these turbines operates with the fluid in the dense vapor thermodynamic state (Thompson, 1971; Romei et al., 2020). Consequently, the value of the optimal solidity prescribed by the available correlations for axial turbines operating with air or steam might lead to a sub-optimal design.

The study aims to investigate the influence of both compressibility and fluid molecular complexity on the optimal solidity of linear turbine cascades. The research documented in this paper represents the first step towards establishing guidelines for the selection of the optimal solidity in the preliminary design of non-conventional turbomachinery (e.g., ORC turbines). Based on Denton's approach (Denton, 1993) and Coull and Hodson's methodology (Coull and Hodson, 2013), a first-principle reduced-order model (ROM) not requiring the use of empirical coefficients was devised to estimate the passage losses as a function of the axial solidity. The resulting charts provide the value of the optimal solidity as a function of the cascade flow angles. Numerical simulations of the flow over an exemplary stator blade were performed to assess the influence of both flow compressibility and axial solidity on the loss breakdown. Optimal solidity values obtained considering passage losses solely and overall losses are compared with the ones resulting from both the ROM and the Zweifel's correlation.

The paper is structured as follows. Section 2 describes the methodology used to derive the reduced-order model and the setup of the numerical simulations. Section 3 reports the numerical analysis results and the charts resulting from the ROM. Finally, section 4 lists the main conclusions drawn from this study and the next steps.

2. METHODOLOGY

The effect of solidity on fluid dynamic performance of turbine cascades can be investigated, either numerically or experimentally, with three different methods: 1) by changing the blade solidity and optimizing its shape for minimum loss at each operating condition (see Doughty et al., 1992); 2) by changing the solidity for a fixed blade shape, but keeping constant the throat-to-spacing ratio for given operating conditions (varying stagger); 3) by solely changing the solidity for a fixed blade shape for varying operating conditions. Because of its simplicity, we adopted the third method in this study.

To assess the influence of the axial solidity σ_x on the fluid-dynamic losses, we performed a set of two dimensional numerical Reynolds Averaged Navier-Stokes (RANS) simulations. Figure 1 shows the computational domain. The blade geometry has been extracted from the stator of the iMM-Kis3 turbine presented in Giuffré and Pini (2021). This turbine stage has been designed to operate with siloxane MM at inlet total temperature and pressure ensuring a compressibility factor of $Z \sim 1$, i.e., in dilute gas conditions. For this analysis, only the fluid-dynamic performance at the mid-span section has been considered.

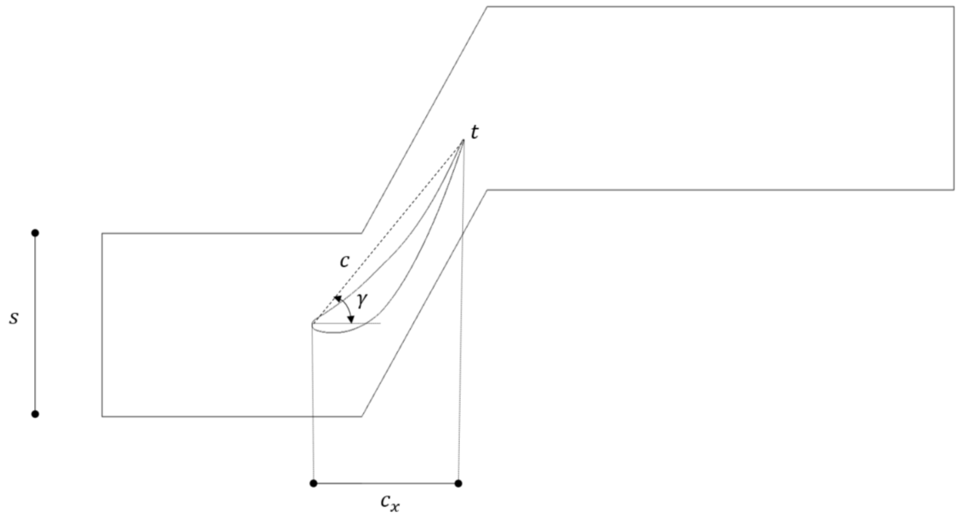

Figure 1: Sketch of the iMM-Kis3 turbine blade and relative flow domain. t denotes the trailing edge thickness.

c [m]	c_x [m]	γ [^{o}]	s [m]	α_m [^{o}]	t [mm]
0.0205	0.0126	50.72	0.0172	68.84	0.054

Table 1: Geometry features of the iMM-Kis3 turbine blade (Giuffré and Pini, 2021). γ, α_m and t denote the blade stagger angle, the blade metal angle at the trailing edge, and the trailing edge thickness, respectively.

Table 1 lists the details of the blade geometry. The baseline design of the stator consists of 42 blades featuring an axial solidity value of $\sigma_{\mathrm{x,ref}} = 0.73$. This value has been calculated using the Zweifel's criterion in the preliminary design phase, see Giuffré and Pini (2021). To avoid upstream effects and enhance mixing downstream of the blade, the inlet and the outlet of the domain have been placed ~ $1.5c_x$ upstream of the leading edge and ~ $3.5c_x$ downstream of the trailing edge, respectively. Two sets of simulations are here considered (see table 2). The two cases differ in the used working fluid: for the iN2 case, the considered fluid is nitrogen, a compound with low complexity of the molecular structure; siloxane MM, an organic compound commonly used in ORC turbogenerators, is considered in the second case, denoted as iMM. In each of the two cases, the inlet total temperature and pressure are prescribed to ensure a compressibility factor of $Z = 1$. To investigate the impact of compressibility effects on the optimal solidity value, three different values of the total-to-static expansion ratio β_{ts} are considered for each case. The first β_{ts} value is representative of a subsonic linear cascade (M_{out} ~ 0.5, M_{out} being the Mach number at the outlet of the domain), the second one of a transonic cascade (M_{out} ~ 1) and the third one of a supersonic cascade (M_{out} ~ 1.2). Finally, for each value of the β_{ts}, 16 different values of the axial solidity ranging from $\sigma_x = 0.5$ to $\sigma_x = 1.45$ are considered. Each σ_x value is obtained by adjusting the pitch value s in the computational domain.

The domain is meshed with quadrilateral elements in the built-on meshing tool of Ansys. A mesh is generated for each value of the axial solidity σ_x, resulting in 16 different meshes in total. To ensure proper resolution, both local refinement in the proximity of the blade walls and average cell size are the same for all meshes. Cell clustering is introduced near the blade walls to guarantee $y^+ < 1$ for all the cases under investigation. Mesh sensitivity analysis conducted on the baseline geometry at $\sigma_x = \sigma_{\mathrm{x,ref}} = 0.73$ resulted in grid independence at 200k cells. Simulations have been run using commercial software (Ansys, 2019). The SST $k - \omega$ model is employed to compute the turbulence stresses. Stagnation pressure, stagnation temperature and turbulent intensity are prescribed at the inlet, according to the values reported in table 2. A turbulent intensity value of 5% and a turbulent viscosity ratio $\mu_\mathrm{T}/\mu = 10$ were used throughout

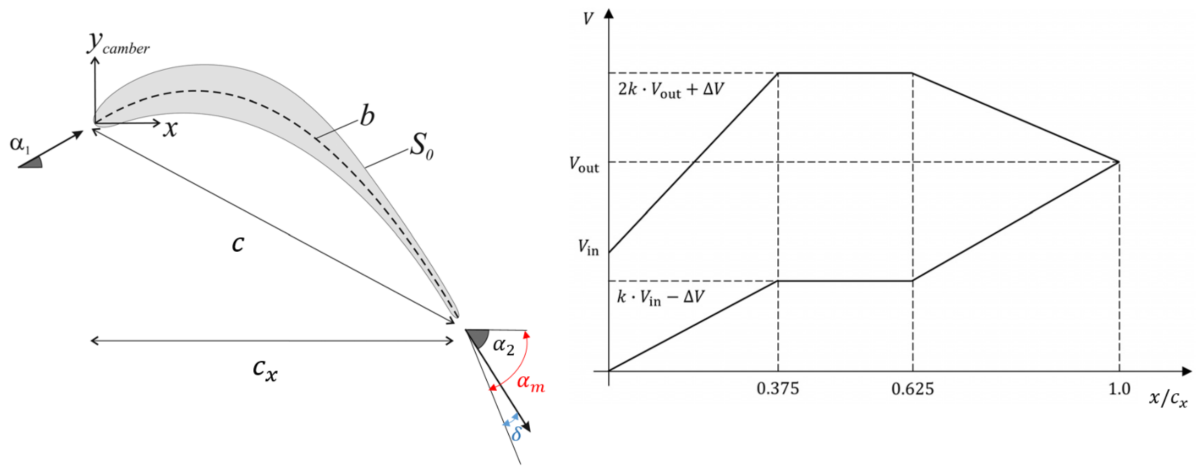

Figure 2: (a) Reference blade geometry for the reduced-order model. Blade thickness is neglected in this study. (b) Simplified velocity distribution along the blade axial direction.

	fluid	M_{mol} [kg/kmol]	γ_∞	p_{t1} [bar]	T_{t1} [K]	$Re_{2,is} \cdot 10^7$	$\beta_{ts,1}$	$\beta_{ts,2}$	$\beta_{ts,3}$
iN2	nitrogen	28	1.4	15	473.15	1.35 – 2.35	1.2	2	2.6
iMM	siloxane MM	162.38	1.025	9.66	534.26	0.63 – 0.83	1.2	1.7	2.2

Table 2: Setup of the cases investigated in the numerical analysis. γ_∞ denotes the ratio of specific heats for $v \to \infty$. The Reynolds number is computed using the blade chord and the isentropic outlet conditions as reference. The last three columns list the values of three total-to-static expansion ratios investigated in each case.

this study. The turbulent Prandtl number is set to $Pr_t = 0.9$, in accordance with Otero R. et al. (2018). The advective and turbulent fluxes are discretized with total variation diminishing schemes. A central difference scheme is used to discretize the viscous fluxes. The fluid properties are calculated with a look-up table approach, resorting to a well-known database for the estimation of thermophysical properties Lemmon et al. (2018).

The optimal σ_x value obtained from the numerical analysis is compared against the ones obtained with both the Zweifel's criterion and a first principle reduced-order model (ROM) accounting for the passage loss as a function of the solidity.

The Zweifel correlation is based on the results of experimental campaigns conducted on subsonic turbine linear cascades. Denoting with α_1 and α_2 the inlet and outlet flow angles and assuming incompressible flow, the correlation by Zweifel reads

$$\sigma_x = \frac{\rho V_x (V_{y2} - V_{y1})}{Z_{Zw} H (p_{t1} - p_2)} = \frac{2\cos^2\alpha_2}{Z_{Zw}} (\tan\alpha_2 - \tan\alpha_1) \,. \tag{2}$$

The development of the ROM has been based on the seminal work of Denton (1993). It is based on a control volume approach over a stationary blade, see figure 2a. Here, we assume a parabolic blade camber with the slope at leading and trailing edge equal to the tangent of the respective flow angles. This results in

$$\frac{y_{camber}}{c_x} = -\frac{x}{c_x}\left(A\frac{x}{c_x} + B\right), \tag{3}$$

with $A = (\tan\alpha_2 - \tan\alpha_1)/2$ and $B = \tan\alpha_1$. To simplify the problem, the blade thickness is set to zero. The velocity distribution over the blade pressure and suction side is the one reported in figure 2b. Here, the unknowns are the parameters k and ΔV. V_{in} and V_{out} are functions of both the axial velocity V_x, which

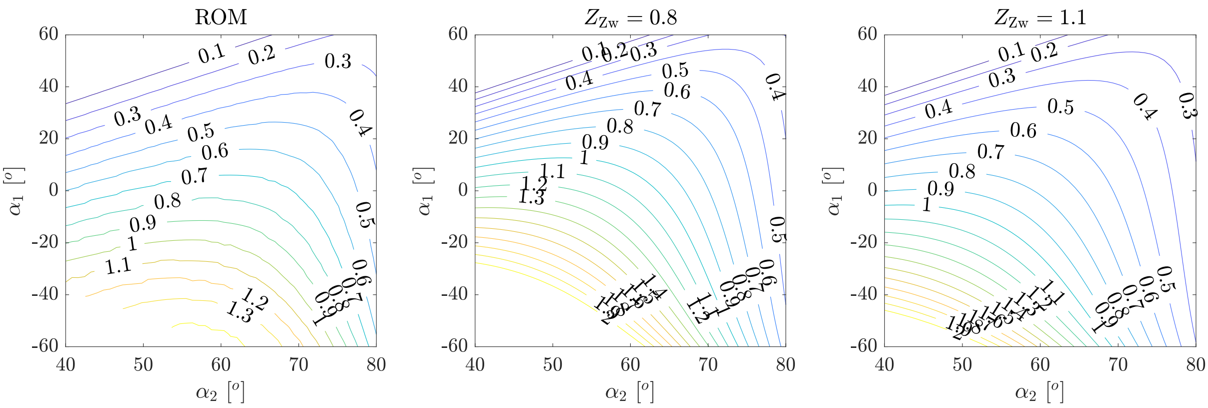

Figure 3: Optimal solidity σ_x *vs* flow angles resulting from (a) reduced-order model, (b)-(c) Zweifel correlation assuming $Z_{Zw} = 0.8$ and $Z_{Zw} = 1.1$, respectively.

is assumed to be constant along the axis, and the flow angles. For incompressible flows, the axial solidity is calculated by combining the relation providing the blade circulation

$$\int_0^1 \left(V_{ss} - V_{ps}\right) \sqrt{1 + \left(2A\frac{x}{c_x} + B\right)^2} \, \mathrm{d}\left(\frac{x}{c_x}\right) = \frac{V_x}{\sigma_x}\left(\tan\alpha_2 - \tan\alpha_1\right), \tag{4}$$

where V_{ss} and V_{ps} are the values of the local absolute velocity along the suction and pressure sides, respectively, with that providing the tangential momentum balance, which yields

$$\int_0^1 \left(V_{ss}^2 - V_{ps}^2\right) \mathrm{d}\left(\frac{x}{c_x}\right) = \frac{2V_x^2}{\sigma_x}\left(\tan\alpha_2 - \tan\alpha_1\right) \tag{5}$$

By minimizing the normalized dissipation due to passage losses, which reads

$$\zeta_{bbl} = \frac{T\dot{S}_{blade}}{1/2\dot{m}V_x^2} = \frac{2C_d\sigma_x}{V_x^3}\int_0^1 \left(V_{ss}^3 - V_{ps}^3\right) \sqrt{1 + \left(2A\frac{x}{c_x} + B\right)^2} \, \mathrm{d}\left(\frac{x}{c_x}\right), \tag{6}$$

C_d being the average boundary layer dissipation coefficient over the blade, one can determine the optimum values of the velocity distribution parameters k and ΔV and, at the same time, the optimum solidity given the inlet and outlet flow angles. According to Denton (1993), we assumed a constant $C_d = 0.002$ value. Unlike Zweifel's correlation, the ROM does not require any empirical closure coefficient, thus ensuring improved accuracy.

3. RESULTS

Figure 3a shows the contours of the optimal solidity as a function of the flow angles calculated with the model described in section 2. The solidity trends reported in this figure are compared with those computed with the Zweifel correlation and reported in figures 3b-c. It can be observed that the optimal σ_x trends are well in agreement regardless of the adopted model. Moreover, the optimal solidity values are found to lie within the bounds obtained with the Zweifel correlation for $Z_{Zw} = 0.8$ and $Z_{Zw} = 1.1$.

Figures 4a-c and 5a-c show the loss breakdown for the iN2 and iMM cases, respectively, processed from the CFD results, for each value of the outlet Mach number corresponding to the β_{ts} reported in table 2. The normalized loss coefficient $\zeta_s = T_2 \mathrm{d}s/u_2^2/2$, where reference temperature and flow velocity are computed at the outlet, is used to quantify the dissipation produced by each loss source. For both cases, the red and the black curves provide the total entropy generation between inlet and outlet of computational domain calculated with the mass-flow and the mixed-out average. The contribution due to passage losses (bbl) is estimated as the mass-flow averaged entropy difference between the inlet section of the computational domain and the station placed in proximity of the trailing edge at $x = 0.98c_x$. The mixing

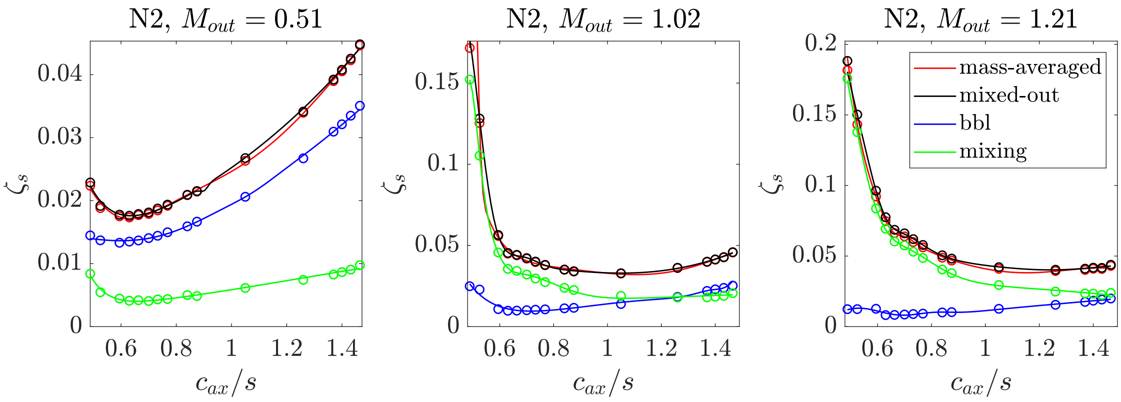

Figure 4: Normalized entropy generation *vs* blade axial solidity for the case iN2. (a) subsonic (b) sonic and (c) supersonic outlet Mach number. The overall loss is computed both with mass-average and mixed-out approaches. Breakdown of mixing and passage (bbl) losses is also provided.

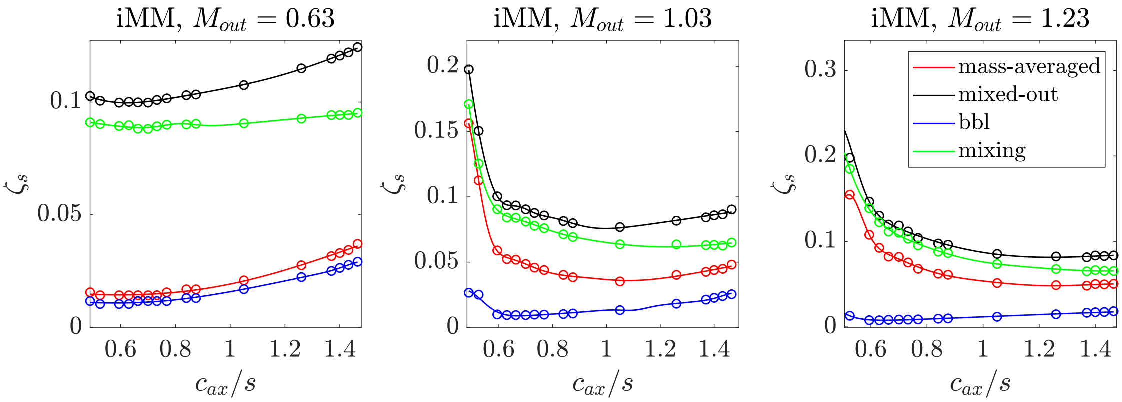

Figure 5: Entropy loss generation *vs* blade axial solidity for the case iMM. (a) subsonic (b) sonic and (c) supersonic outlet Mach number. The overall loss is computed both with mass-average and mixed-out approaches. Breakdown of mixing and passage (bbl) losses is also provided.

loss is finally obtained by subtracting the passage loss contribution from the mixed-out one. All the results point out that the optimal solidity value increases with flow compressibility or, similarly, with the cascade Mach number, regardless of the adopted working fluid. Conversely, passage losses exhibit a minimum at $\sigma_x \sim 0.65$, and this value is found to be not affected by flow compressibility, as already highlighted by Denton (1993). At subsonic operating conditions (figures 4a and 5a), passage losses prevail over the mixing losses. Consequently, the overall minimum loss (either mixed-out or mass-averaged) is found at $\sigma_x \sim 0.65$ for both cases. At higher values of M_{out}, mixing losses increase and become the most dominant loss source for the case at highest Mach number (figures 4c and 5c). Because of that, the optimal solidity value becomes more sensitive to the trend of mixing losses for cascades operating at $M_{\text{out}} > 1.2$, for both working fluids. In the highly transonic case (figures 4c and 5c), the optimal solidity value is ~ 1.2.

The physical reason underlying the variation of mixing losses as function of the solidity can be determined by inspecting the entropy contours displayed in figures 6a-c, which refer to the iMM case at $\beta_{\text{ts}} = 1.7$ or, equivalently, $M_{\text{out}} \sim 1$. At $\sigma_x \sim 0.65$ (figure 6a), passage losses are minimized because of the low overall wetted area. Furthermore, the poor flow guidance provided by the blades causes a high flow diffusion on the rear part of the suction side, which entails a considerable boundary layer growth in the vicinity of the trailing edge. As a result, mixing losses becomes significant because of the combined effect of wake mixing at the trailing edge and diffusing boundary layer. At high $\sigma_x \sim 1.05$ (figure 6b), the wetted surface increases, leading to an increase of passage losses. In contrast, mixing losses decrease

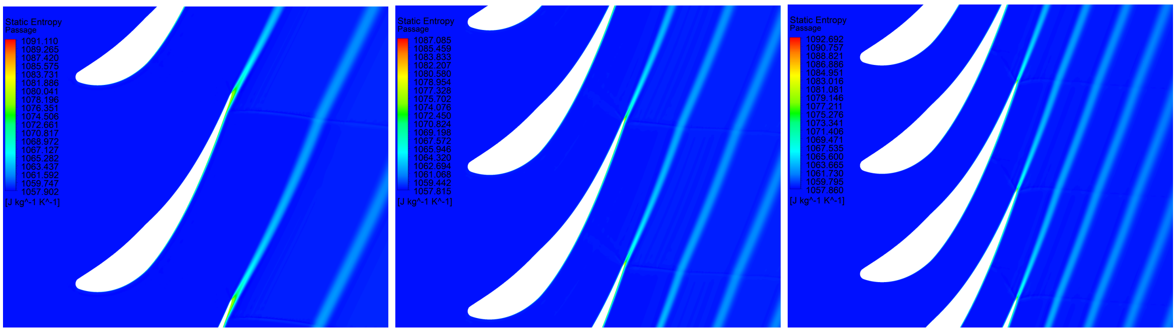

(a) $\sigma_x = 0.65$ **(b)** $\sigma_x = 1.05$ **(c)** $\sigma_x = 1.4$

Figure 6: Entropy field in proximity of the blade trailing edge for the case iMM, $\beta_{ts} = 1.7$.

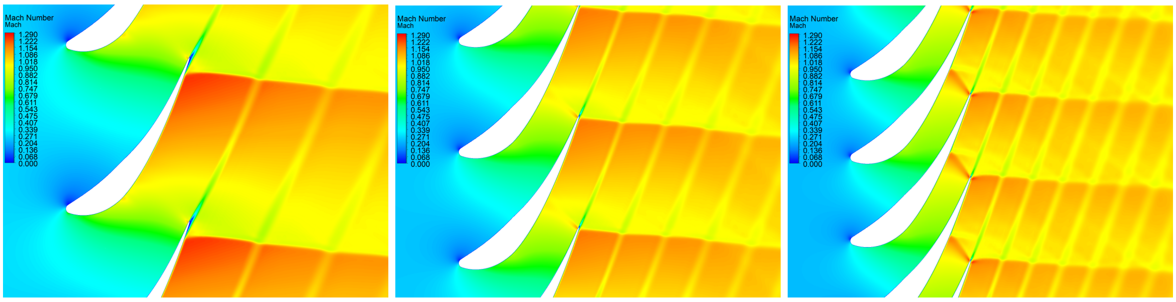

(a) $\sigma_x = 0.65$ **(b)** $\sigma_x = 1.05$ **(c)** $\sigma_x = 1.4$

Figure 7: Mach number field in proximity of the blade trailing edge for the case iMM, $\beta_{ts} = 1.7$.

as a consequence of the improved flow guidance. However, at $\sigma_x \sim 1.4$ (figure 6c), the increase of the number of wakes mixing with the bulk flow causes a progressive increase of the associated loss. The same physical explanation, albeit with the different share of the losses, also applies for the highly transonic cases. The effect of the solidity on the wake at the blade trailing edge is also visible in the Mach number contours, see figure 7. The Mach number contour plots also highlight the presence of a shock wave in proximity of the trailing edge.

Figure 8a shows the flow deviation as a function of the cascade solidity for all the investigated cases. The deviation decreases with the solidity and, conversely, increases with the cascade M_{out}, i.e., with the flow compressibility. Higher flow deviation implies more significant mixing losses, in agreement with what has been previously discussed. Finally, figure 8b illustrates the trend of the optimal solidity value as a function of the M_{out} for the considered test cases. Values of optimal σ_x as function of the overall loss and the passage loss only are reported in the chart. The optimal solidity values calculated with Zweifel's criterion assuming $Z_{Zw} = 0.85$, $Z_{Zw} = 0.95$ and $Z_{Zw} = 1.1$, and that estimated by the model described in section 2 are also depicted. For both models, $\alpha_2 = \alpha_m$, α_m being the outlet blade metal angle. For transonic and supersonic flows, both ROM and Zweifel's correlations do not return the same optimal solidity value minimizing the overall loss that numerical simulations have provided. This is due to the inherent limitations of both models, which account for the passage loss only and rely on the incompressible flow assumption. Regarding the effect of the working fluid on the optimal solidity, lower values are obtained for the cascades operating with siloxane MM than those operated with nitrogen, if $M_{out} < 1$. At higher M_{out}, the impact of the working fluid seems to be minor.

4. CONCLUSION

The influence of both molecular complexity of the working fluid and flow compressibility on the optimal solidity of turbine cascades has been investigated. The optimal solidity values provided by Zweifel's criterion have been compared against those obtained from a first-principle reduced-order model and nu-

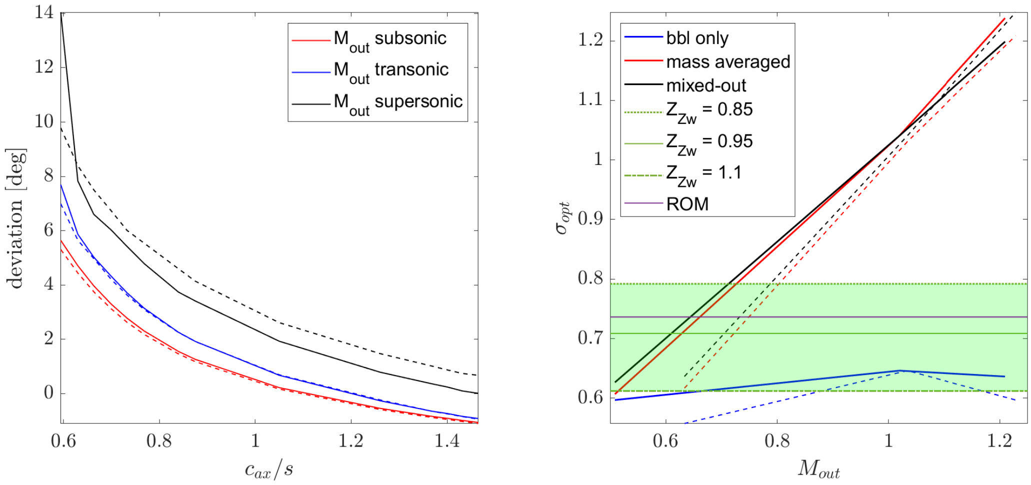

Figure 8: (a) Flow deviation at blade trailing edge *vs* axial solidity for the investigated cases. (b) optimal solidity *vs* outlet Mach number for the investigated cases. The value predicted by the reduced-order model (ROM) and the Zweifel correlation for three different values of the Z_{ZW} are also displayed. The region of validity of the Zweifel correlation for $Z_{\mathrm{ZW}} = 0.8 - 1.1$ is also highlighted. In both graphs, solid and dotted lines refer to the iN2 and iMM cases, respectively.

merical simulations of the flow around an ORC turbine stator. A loss breakdown analysis has been carried out to gain physical insights. Based on the results of the study, we can draw the following conclusions.

- Results from numerical simulations show that both the Zweifel's correlation and the reduced-order model provide inaccurate values of the optimal solidity because they do not account for mixing losses.
- The higher the cascade outlet Mach number, the higher the optimal solidity value, regardless of the fluid.
- For transonic and supersonic cascades, the influence of the working fluid on the optimal solidity value is arguably negligible.

The research documented in this paper is the first step towards developing new design guidelines for the selection of the optimal solidity in axial and radial ORC turbines. Future efforts will involve the extension of the ROM to include mixing losses, the implementation of a model for the calculation of the dissipation coefficient C_{d} in equation 6 as described in Pini and De Servi (2020), and the use of a more accurate methodology for the evaluation of the optimal solidity based on the approach described by Doughty et al. (1992). Verification of the numerical results obtained with other turbulence models will also be performed.

5. ACKNOWLEDGMENT

This research has been supported by the Applied and Engineering Sciences Domain (TTW) of the Dutch Organization for Scientific Research (NWO), Technology Program of the Ministry of Economic Affairs, grant # 15837.

REFERENCES

I. Ansys. Ansys CFX release 19.1, 2019.

J. D. Coull and H. P. Hodson. Blade Loading and Its Application in the Mean-Line Design of Low

Pressure Turbines. *Journal of Turbomachinery*, 135(2):021032, Mar. 2013. ISSN 0889-504X, 1528-8900. doi: 10.1115/1.4006588.

J. D. Denton. The 1993 IGTI scholar lecture: Loss mechanisms in turbomachines. *Journal of Turbomachinery*, 115(4):621–656, 10 1993. ISSN 0889-504X. doi: 10.1115/1.2929299.

R. Doughty, H. Moses, and B. Gregory. The effect of blade solidity on the aerodynamic loss of a transonic turbine cascade. In *30th Aerospace Sciences Meeting and Exhibit*, Reno,NV,U.S.A., Jan. 1992. American Institute of Aeronautics and Astronautics. doi: 10.2514/6.1992-393.

A. Giuffré and M. Pini. Design Guidelines for Axial Turbines Operating With Non-Ideal Compressible Flows. *Journal of Engineering for Gas Turbines and Power*, 143(1):011004, Jan. 2021. ISSN 0742-4795, 1528-8919. doi: 10.1115/1.4049137.

E. W. Lemmon, , I. H. Bell, M. L. Huber, and M. O. McLinden. NIST standard reference database 23: Reference fluid thermodynamic and transport properties-REFPROP, version 10.0, National Institute of Standards and Technology, 2018.

G. J. Otero R., A. Patel, R. Diez S., and R. Pecnik. Turbulence modelling for flows with strong variations in thermo-physical properties. *International Journal of Heat and Fluid Flow*, 73:114–123, Oct. 2018. ISSN 0142727X. doi: 10.1016/j.ijheatfluidflow.2018.07.005.

M. Pini and C. De Servi. Entropy generation in laminar boundary layers of non-ideal fluid flows. *Non-Ideal Compressible Fluid Dynamics for Propulsion and Power: Lecture Notes in Mechanical Engineering*, pages 104–117, 2020. doi: 10.1007/978-3-030-49626-5_8.

A. Romei, D. Vimercati, G. Persico, and A. Guardone. Non-ideal compressible flows in supersonic turbine cascades. *Journal of Fluid Mechanics*, 882, Jan. 2020. ISSN 0022-1120, 1469-7645. doi: 10.1017/jfm.2019.796.

P. A. Thompson. A Fundamental Derivative in Gasdynamics. *Physics of Fluids*, 14(9):1843, 1971. ISSN 00319171. doi: 10.1063/1.1693693.

W. Traupel. *Thermische Turbomaschinen*. Springer Berlin Heidelberg, 1966. ISBN 978-3-662-13209-8.

O. Zweifel. *The Spacing of Turbo-Machine Blading Especially with Large Angular Deflection*. Brown Boveri Review, 1945.